FLEXIBILITY AND ECONOMIC DISPATCH OF ISLAND POWER SYSTEMS WITH INTEGRATED THERMAL ENERGY STORAGE IN SMART GRIDS

Panagiotis Romanos[1,*], Emmanouil Voumvoulakis[2] Christos N. Markides[3], Nikos Hatziargyriou[1,2]

[1]National Technical University of Athens, School of Electrical and Computer Engineering, Athens, Greece
takis.romanos@gmail.com, nh@power.ece.ntua.gr

[2]Hellenic Electricity Distribution Network Operator, Athens, Greece
E.Voumvoulakis@deddie.gr

[3]Clean Energy Processes (CEP) Laboratory, Department of Chemical Engineering,
Imperial College London, London, UK
c.markides@imperial.ac.uk

* Corresponding Author

ABSTRACT

The increasing penetration of intermittent renewable energy generation into the grid poses a number of challenges, including a high demand for flexibility. In this paper, the provision of flexible power generation is investigated by extracting steam from steam (Rankine-cycle) power stations during off-peak demand in order to charge thermal energy storage (TES) tanks that contain suitable phase-change materials (PCMs); at a later time, when this is required and/or is economically effective, these TES tanks can act as the heat sources of secondary thermal power plants to generate power, for example as evaporators of organic Rankine cycle (ORC) plants that are suitable for power generation at reduced temperatures and smaller scales. This solution offers greater flexibility than TES-only technologies that store thermal energy and release it back to the base power-station, since it allows both derating but also over-generation compared to the base power-station capacity. The solution is applied in a case study of a 50-MW rated oil-fired power station in the autonomous electrical system of Crete. In this island system, oil-fired power stations are used for delivering so-called ‘base load’ power, while their output can follow the load demand. It is found, through a thermodynamic analysis, that a maximum combined power of 70 MW can be delivered during peak demand, which is 40% higher than the oil-fired plant’s full-load rating. The scenario also allows a maximum plant derating of 74%, i.e., down to 13 MW during off-peak demand, which is significantly lower compared to the minimum stable generation of 27 MW. In such a scheme, a suitable energy management system (EMS) is needed to optimize the derating of these power stations for charging the thermal tanks during off-peak demand and to control the discharging of the tanks for electricity generation from the secondary plants during peak demand. The optimal operation of the TES system is investigated, by solving a modified Unit Commitment – Economic Dispatch optimization problem, which includes the constraints and techno-economic characteristics of the TES. The annual operation of the power system of Crete projected to the year 2020, with and without the installation of the TES, is simulated for several scenarios and a cost benefit analysis is performed based on the comparative results of the simulations. The results indicate that, for most of the scenarios, the discounted payback period is below 12 years, while in a few cases the payback is as low as 5 years.

1. INTRODUCTION

The decarbonisation of the electricity system requires significant and continued investment in low-carbon and renewable energy sources. With the diminishing output and shorter operating hours of conventional power plants, the system inertia reduces and there is a growing need and opportunity for distributed energy resources (DERs) to contribute to the provision of system balancing, flexibility and security to support a cost-effective transition to a lower-carbon energy system.

Coal-fired power stations often represent a large share of the power delivered to grids, and therefore their management can be used to improve grid stability with great effectiveness in the scenario of a significant generation of intermittent renewable electricity. An interesting option, for example, involves the conversion of heat to electricity at peak-demand times by integrating waste heat in the feedwater preheating systems of such plants, as investigated by Roth et al. [1] in a 390-MW coal-fired power plant. Thermal energy storage (TES) integration into coal-fired power plants is often proposed as a promising solution for enhanced flexibility and load-following operations, as in Richter et al. [2]. The present study also considers generation-integrated TES, and is readily extended to coal-fired power stations.

The present work goes beyond a previous study [2] that investigated thermal integration with stores in the preheating routes of power stations, by: (i) considering different configurations and strategies for integrating TES in power stations; (ii) developing load-following operations directly applicable to steam power stations, and in particular oil-fired power stations; and (iii) considering the conversion of the stored thermal to electrical power via ORC plants for connection to transmission networks.

2. POWER STATIONS WITH INTEGRATED THERMAL ENERGY STORAGE

2.1 Case-Study Base Power-Station

Figure 1 presents an outline of the main components of the oil-fired power station operating in the autonomous power system of Crete that is used as a study case together with the corresponding thermodynamic processes. The working fluid undergoes the following processes [3,4]:

- *Process 1-2*: Expansion of the working-fluid vapour (steam) through the high-pressure turbine (HPT) and heat is converted to work $W_{\mathrm{el\_1}}^{\mathrm{t}}$;
- *Process 2-3*: Expansion through the low-pressure turbine (LPT) to the condenser pressure and work generation $W_{\mathrm{el\_2}}^{\mathrm{t}}$ (the total work $W_{\mathrm{el}}^{\mathrm{t}}$ is the sum of work $W_{\mathrm{el\_1}}^{\mathrm{t}}$ and work $W_{\mathrm{el\_2}}^{\mathrm{t}}$);
- *Process 3-4*: Heat transfer at constant pressure through the condenser to saturated liquid State 4;
- *Process 4-5*: Pressurization of the saturated working-fluid liquid in the feed pump;
- *Process 5-1*: Isobaric heat addition through the boiler to complete the cycle within a range of minimum stable operation and maximum output ($Q_{\mathrm{boil}}^{\mathrm{max}}$, $Q_{\mathrm{boil}}^{\mathrm{min}}$).

The thermal input to the power station is 123 MW (128 MW fuel input), the electrical power output is 50 MW and the thermal efficiency of the cycle is 39.2%. The isentropic efficiencies of the HPT and LPT are 70% and 75%, respectively. The electrical power consumption of the feedpump is 0.9 MW and its isentropic efficiency is 78% [5]. We consider the integration of TES into this power station with the aim of modulating its power output and reducing its minimum stable generation.

2.2 Thermal-energy store charging

The charging characteristics of thermal stores depend strongly on the materials used. In the investigated TES schemes, materials selection is determined by the temperature at which steam is extracted at various points from the case-study oil-fired power station. The following steam-extraction possibilities are considered: (i) before the HPT at 530 $^{\mathrm{o}}$C and 100 bar or from the glands of the HPT, and/or (ii) before the LPT at 198 $^{\mathrm{o}}$C and 2.4 bar. In this study we investigate TES with steam extraction before the HPT, since the thermal stored energy is the maximum.

As illustrated in Fig. 1, the working fluid undergoes the following series of processes:

- *Process 1-a*: Diversion of part of the working fluid (superheated steam) flow upstream of the HPT $Q_{\mathrm{cond}}^{\mathrm{t}}$ followed by isobaric heat rejection and condensation of the steam flow, while charging a first PCM thermal-tank (Thermal Tank 1);
- *Process a-b*: Isobaric heat rejection while charging a second PCM thermal-tank (Thermal Tank 2) (the total thermal energy stored in both thermal tanks is denoted as $Q_{\mathrm{stor}}^{\mathrm{t}}$);
- *Process b-5:* Pressurization of the subcooled working-fluid (water) in a feedpump and return of the diverted flow to the main plant boiler.

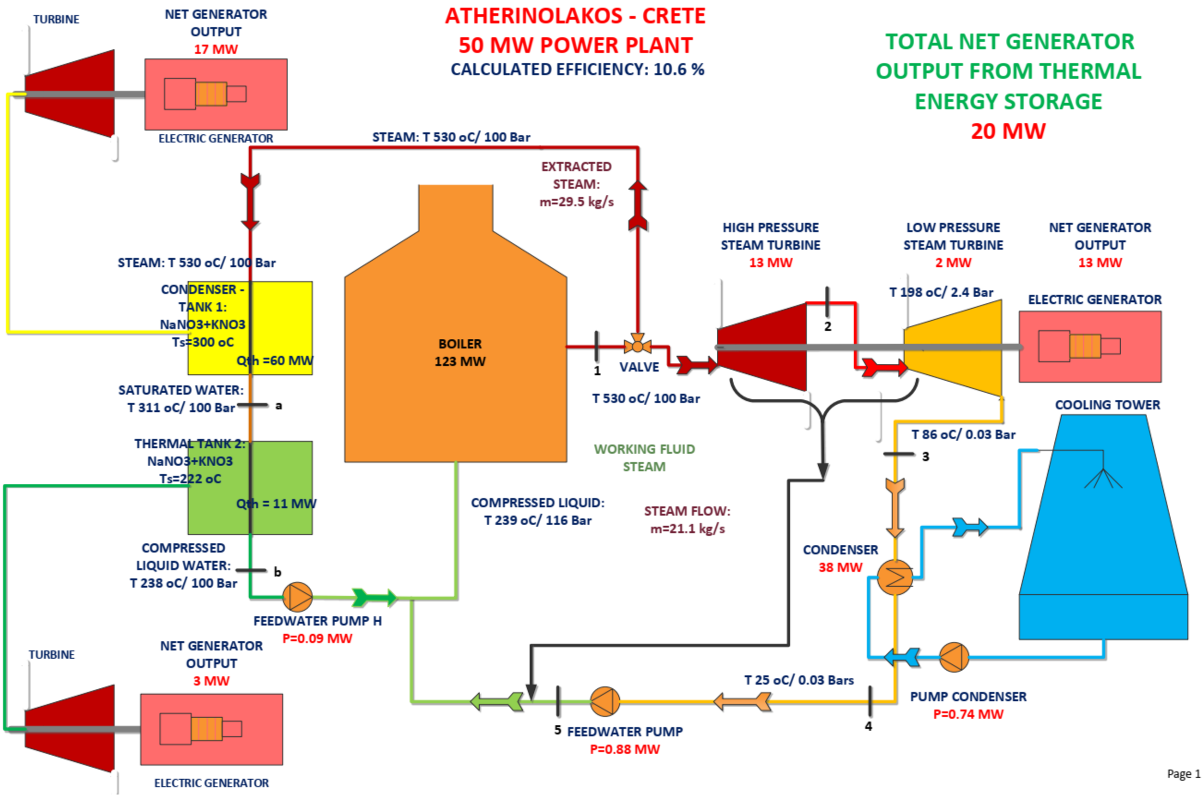

Figure 1: Integration of two PCM-based TES tanks in the Atherinolakos PPC oil-fired power station in Crete, with steam extracted before the high-pressure turbine[1].

As a guideline for this particular power station, an allowable steam-extraction rate of up to 29.5 kg/s for diversion before the HPT to Thermal Tank 1 (and also Thermal Tank 2, which is in series with the first tank; see Fig. 1) is considered. This represents 60% of the total steam passing to the HPT under normal conditions. As a result, thermal energy can be stored in Thermal Tank 1 at a maximum heat transfer rate of 60 MW and in Thermal Tank 2 at a rate of 11 MW during the charging of these stores. Assuming a 50% depth of discharge, the calculated volumes of Thermal Tanks 1 and 2 are 2000 m^3/60 MWh and 375 m^3/11 MWh, respectively.

Our analysis is based on state-of-the-art PCM mixtures found in CSP applications. In more detail, superheated steam at 530 ^oC (and 100 bar) is extracted before the HPT and condensed isobarically in Thermal Tank 1 to a stream of saturated liquid water at 311 ^oC (100 bar). The storage medium in this tank is a PCM mixture of potassium and sodium nitrates ($NaNO_3$+KNO_3) with a melting point of 300 ^oC [6], which is just below the minimum temperature of the steam in the tank. Downstream, and in series with Thermal Tank 1, heat transfer also occurs to Thermal Tank 2 where the condensed, high-pressure (initially saturated) stream cools further, again isobarically as it charges this second tank. The inlet temperature of this tank is 311 ^oC (at 100 bar) and the outlet 238 ^oC (at 100) bar. This tank also employs a PCM mixture of potassium and sodium nitrates but with a different composition so that its melting point is at 222 ^oC, which is (as in Thermal Tank 1) just below the minimum temperature in this tank.

Finally, after the two TES tanks, the subcooled liquid (water) is compressed in a feedpump and returned to the boiler. The electrical power consumption of the additional feedpump is estimated at 0.09 MW, by assuming an isentropic efficiency value of 80% for this component. The partial diversion of the steam flow to the high pressure turbine during the charging of the two cascaded thermal tanks, leads to a drop in the thermal input of the power station (from 123 MWth; see Fig. 1) to

[1]For simplicity, multiple bleed points from the turbines for regenerative feedheating are denoted in this figure by a single line connecting the turbines to the output of the feedwater pump

52 MWth, as the electrical power output of the power plant is derated by 74% (from 50 MWe) to 13 MWe and the corresponding thermal efficiency of the plant is reduced (from 39.2%) to 10.6%.

2.3 Thermal-energy store discharging

During TES discharging, heat is delivered from the TES tanks to ORC engines for secondary power generation. The ORC engines considered here are based on subcritical and recuperative cycles, and comprise the following key components: (i) the integrated TES-evaporator heat exchanger (HEX), where heat is added to the cycle from the PCM in the thermal stores; (ii) the expander/turbine where power is generated; (iii) the recuperator HEX, where the (hot) desuperheating working fluid vapour exchanges heat with the (cold) working fluid leaving the pump; (v) the condenser HEX, where heat is rejected to a cooling circuit; and (v) the pump, which maintains the working fluid circulation in the engine. Based on observations from previous studies [7], these ORC engines have not been modelled in detail here, but rather their thermal efficiency is estimated based on both reversible and endoreversible analyses; of particular interest are the latter, which have been shown to provide efficiency predictions with a degree of accuracy that is considered sufficient for the present work.

In more detail, similarly to the Carnot (reversible) heat engine, the Novikov (endoreversible) heat engine is based on a constant source/storage tank temperature, $T_{\mathrm{h}} = T_{\mathrm{st}}$, and a constant sink/ambient temperature, $T_{\mathrm{c}} = T_{\mathrm{a}}$. The Carnot and Novikov efficiency expressions are:

$$\eta_{\mathrm{C}} = 1 - \frac{T_{\mathrm{a}}}{T_{\mathrm{st}}} \tag{1}$$

$$\eta_{\mathrm{N}} = 1 - \sqrt{\frac{T_{\mathrm{a}}}{T_{\mathrm{st}}}} \,. \tag{2}$$

In both cases (Carnot and Novikov), a measure of thermal efficiency can be used to obtain the generated electrical power, $\dot{W}_{\mathrm{cycle}}$ or P_{out}, from an engine given a thermal-energy input rate, $\dot{Q}_{\mathrm{in}}$, via Eq. (3):

$$\eta_{\mathrm{th}} = \frac{\dot{W}_{\mathrm{cycle}}}{\dot{Q}_{\mathrm{in}}} \Rightarrow \dot{W}_{\mathrm{cycle}} = \eta_{\mathrm{th}} \cdot \dot{Q}_{\mathrm{in}} \,, \tag{3}$$

where η_{th} can be either η_{C} or η_{N}, and the sink for the secondary power plants is the environment.

Table 1: Summary of ideal cascaded TES results and secondary power-plant outputs when steam is extracted before the high-pressure turbine.

	Thermal Tank 1	Thermal Tank 2
Heat rate input (MWth)	60	11
Reversible (Carnot) efficiency (%)	48	40
Reversible electrical power (MW)	29	4
Endoreversible (Novikov) efficiency (%)	28	22
Endoreversible electrical power P_{out} (MW)	17	3

It is noted that the heat rejection rate at the condenser is reduced from 72 MW, when the oil-fired power plant operates as usual, to 38 MW (see Fig. 1) when steam is extracted before the high-pressure turbine. In effect, this reduced condensation (and waste-heat rejection to the environment) compensates the increased thermal energy that is sent to the secondary power units, which are relatively efficient in converting this to electrical power. This allows a secondary power generation during the discharging of all Thermal Tanks of 20 MW (endoreversible) for a drop in base generation during charging of 13 MW (see Table 1), corresponding to effective round-trip efficiencies of around 56%.

3. RESULTS FOR THE OIL-FIRED POWER STATION CASE STUDY

Figure 2a shows the fractional plant derating during TES charging versus the degree of steam extraction when steam is extracted before the HPT to the oil-fired power station case study.

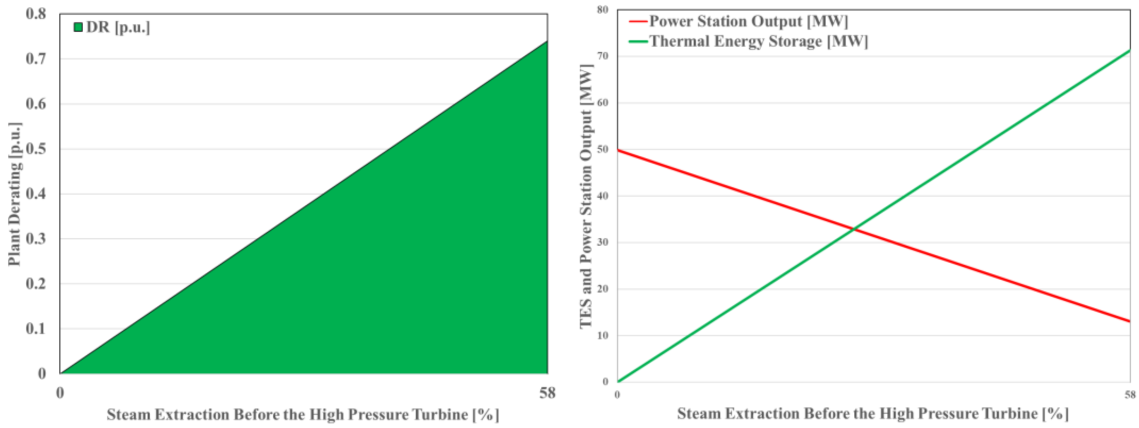

(a) **(b)**

Figure 2: a) Fractional plant derating, and b) power output of main/base oil-fired power station and stored thermal energy during TES charge, for the steam extracted before the high-pressure turbine.

The fractional derating value is the ratio of the net generator output from the base plant with steam extraction to that without steam extraction, i.e., with a maximum net generator output of 50 MW from the base power plant. As a result of these steam extraction strategies, the electrical power output of the power station reduces and the amount of stored thermal energy increases (from left to right in Fig. 2b). This figure suggests that it is possible to use existing oil-fired power plants for flexible power generation in load following with a maximum derating of 74%, with minimum loads down to 26% of the plant's rating. The stored thermal energy increases with the amount of steam extraction up to a total of 71 MW, as the net power output reduces by 74%, from 50 MW to a minimum stable generation of 13 MW. It is interesting to note that the greatest flexibility of the power station, and therefore the largest potential for load following operations, is attained for high-temperature TES at 300 °C. Fig. 3a shows the heat input (rate) to the plant and Fig. 3b the plant efficiency during TES charging for the same steam extraction scheme, as in Fig. 2. The heat input is maximum when steam is not extracted, while it reduces with the amount of steam extraction. As a result of the steam extraction, the thermal efficiency of this particular oil-fired plant reduces from 39.2% (for full-load plant operation) to 10.6% (for 26% part-load operation).

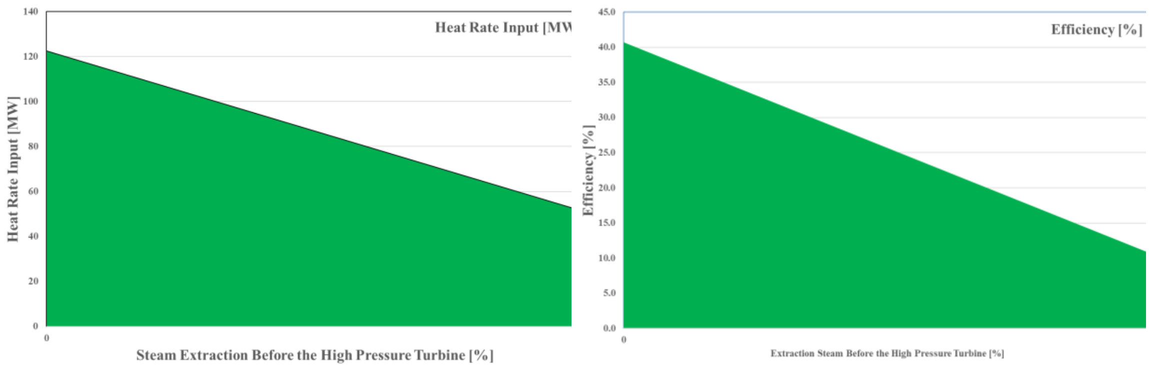

(a) **(b)**

Figure 3: a) Heat input (rate), and b) efficiency of main/base oil-fired power station during TES charge, corresponding to the same EMS schemes as in Fig. 2.

4. OPTIMAL SCHEDULLING IN THE POWER SYSTEM OF CRETE

In this section the optimal scheduling of the TES, i.e. optimal charging/discharging during the day, is examined within the power system of Crete. Crete is the largest Greek island and the 5th largest in the Mediterranean Sea with an annual peak load around 700 MW (for 2018). RES are a vital part of Crete's power system with around 200 MW of wind power and 100 MW of PV plants installed [8]. Three thermal power stations comprising number of oil-fired generating units (diesel, gas turbines, steam turbines and one combined-cycle unit) with around 708 MW total capacity are installed in the power system. Compliance to environmental directives 2010/75/EU (IED) [9] and 2015/2193/EU (MCPD) [10] require the decommissioning of a number of local units leading to generating capacity shortage. An AC interconnection with the mainland system with a net transfer capacity of around 180 MW is planned for completion in the next few years to reduce the high operating cost, increase RES penetration levels and improve reliability and generation adequacy of the system. The integration of the TES in the power system of Crete could have various potential benefits in the following areas: a) energy arbitrage, b) ancillary services, c) avoidance of renewable curtailment, d) unit flexibility, and e) generating capacity.

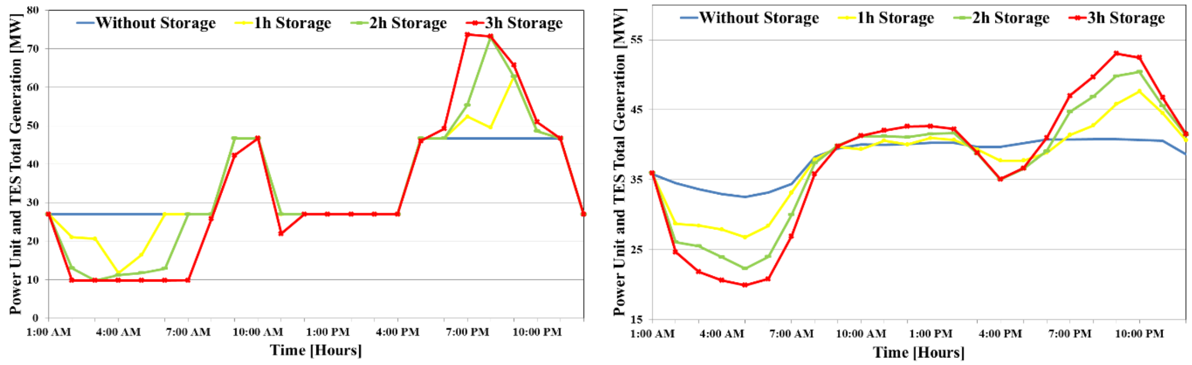

Figure. 4: a) Daily Operation of the TES system for the scenario of interconnected operation of power system of Crete with low fuel prices and low load for a random day, and b) average Annual Operation of the TES system for the scenario of interconnected operation of power system of Crete with low fuel prices and low load for a random day.

In order to quantify the potential benefit of the operation of the TES in the power system of Crete, an optimal scheduling is defined by solving the unit commitment – economic dispatch (UC-ED) optimization problem which is employed in order to integrate the operating constraints imposed by the TES. The UC-ED optimization formulation is used to simulate the operation of the system projected to the year 2020 for an annual period using as inputs the techno economic data of power units, time series of load and RES generation as well as adjusted historical data for the marginal prices of the Greek mainland system. The analysis takes into account the maintenance schedule of generation system as well as stochastic outages according to the expected forced outage rates (EFOR) of the power units. A number of cases are investigated, characterized by differences in the operation of the interconnection to the mainland power system (interconnected and autonomous operation), the fuel prices (low, baseline and high price scenarios), the load demand (low and high load assumptions) and the storage capacity (1, 2 and 3 hours capacity).

Figure 4a illustrates the aggregate electrical output of the steam unit together with the attached TES system for a random day for the scenario of interconnected operation with low fuel prices and baseline load demand and Figure 4b shows the average annual aggregate electrical output of the steam unit together with the attached TES system. According to these figures, the integration of thermal-energy storage into the power station leads to a more flexible operation of the power unit, as expected, which stores energy during valley hours and gives it back to the system at peak demand.

The results of the analysis are presented in Table 2. A value of lost load (VOLL) of 2,000€/MWh has been assumed to calculate the cost of ENS. The total cost of each scenario is defined as the sum of fuel cost, start-up cost (SUC) and ENS cost. It has been assumed that the installation cost for 1 hour of storage is 23.5 M€, for 2 hours is 27 M€ and for 3 hours is 30.5 M€, according to [11,12]. The equivalent annual cost of the installation is 2.4 M€, 2.75 M€ and 3.105 M€ respectively, considering a discount rate of 8% for a lifetime period of 20 years.

Table 2: Results of annual simulation of the scenarios under study.

	Load	Fuel Prices	Storage	Fuel Cost (M€)	SUC (M€)	ENS (MWh)	Total Cost (M€)	TES (MWh)	Discounted Payback Period (years)	(Annual Cost) vs Potential Benefit of TES operation(k€)
Autonomous	Low	Low	-	277,1	6,3	2.202	287,7	-		
			1 Hour	273,3	5,5	1.175	281,2	13.658	4,4	(2400) 6586
			2 Hours	271,9	5,3	1.155	279,5	22.873	4	(2750) 8237
			3 Hours	271,2	5,3	1.153	278,8	29.654	4,2	(3105) 8950
		Baseline	-	329,5	6,4	2.221	340,4	-		
			1 Hour	324,9	5,7	1.177	332,9	14.087	3,8	(2400) 7468
			2 Hours	323,3	5,6	1.160	331,2	23.256	3,5	(2750) 9234
			3 Hours	322,5	5,5	1.166	330,4	30.225	3,7	(3105) 10042
		High	-	382,5	6,5	2.235	393,5	-		
			1 Hour	376,5	5,9	1.189	384,8	14.035	3,2	(2400) 8749
			2 Hours	375,0	5,8	1.162	383,1	23.055	3,1	(2750) 10381
			3 Hours	373,8	5,7	1.153	381,8	30.260	3,1	(3105) 11733
	High	Low	-	304,4	7,2	4.894	321,5	-		
			1 Hour	301,0	6,5	2.618	312,7	14.380	3,2	(2400) 8718
			2 Hours	299,8	6,4	2.610	311,4	23.387	3,2	(2750) 10080
			3 Hours	299,0	6,4	2.617	310,6	30.325	3,4	(3105) 10805
		Baseline	-	362,4	7,4	4.855	379,5	-		
			1 Hour	358,3	6,6	2.607	370,1	14.700	2,9	(2400) 9446
			2 Hours	356,7	6,5	2.598	368,4	23.953	2,9	(2750) 11115
			3 Hours	356,0	6,4	2.603	367,6	30.786	3	(3105) 11940
		High	-	420,6	7,5	4.859	437,8	-		
			1 Hour	415,7	6,9	2.630	427,8	14.810	2,8	(2400) 9981
			2 Hours	414,2	6,7	2.637	426,2	23.938	2,7	(2750) 11539
			3 Hours	413,2	6,6	2.650	425,0	30.760	2,8	(3105) 12753
Interconnected	Low	Low	-	173,6	5,4	55	179,1	-		
			1 Hour	170,9	5,4	2	176,3	7.010	14,7	(2400) 2786
			2 Hours	170,0	5,3	3	175,3	11.025	10,9	(2750) 3824
			3 Hours	169,8	5,1	3	174,9	13.612	11,5	(3105) 4157
		Baseline	-	190,8	6,4	43	197,4	-		
			1 Hour	188,1	6,2	1	194,3	6.973	12,5	(2400) 3063
			2 Hours	187,3	6,0	3	193,3	11.082	10	(2750) 4042
			3 Hours	186,6	5,9	4	192,5	14.031	9	(3105) 4883
		High	-	208,2	7,4	47	215,7	-		
			1 Hour	204,5	7,3	4	211,8	7.072	8,7	(2400) 3869
			2 Hours	203,4	6,7	4	210,2	11.043	6,5	(2750) 5513
			3 Hours	203,1	6,6	3	209,7	13.813	6,8	(3105) 6013
	High	Low	-	190,1	5,6	193	196,1	-		
			1 Hour	187,5	5,6	47	193,2	7.833	13,7	(2400) 2894
			2 Hours	186,9	5,5	46	192,5	12.876	12,2	(2750) 3550
			3 Hours	186,6	5,4	47	192,1	15.880	12,3	(3105) 3994
		Baseline	-	211,1	6,7	183	218,2	-		
			1 Hour	208,0	6,7	50	214,8	7.967	10,6	(2400) 3384
			2 Hours	207,2	6,4	54	213,7	12.408	8,5	(2750) 4502
			3 Hours	206,9	6,3	47	213,3	15.739	9	(3105) 4903
		High	-	231,4	7,7	187	239,4	-		
			1 Hour	227,6	7,7	54	235,4	8.150	8,1	(2400) 4068
			2 Hours	226,7	7,2	50	233,9	12.763	6,6	(2750) 5485
			3 Hours	226,4	7,0	50	233,5	15.560	7	(3105) 5909

The results from Table 2 indicate that the benefit of the installation of a TES in the power system of Crete lies in the range of 2.7 to 6.0 M€/annum assuming the interconnected operation of the system and from 6.5 to 12.7 M€/annum for the autonomous operation. The benefit increases for high fuel prices and high demand. The largest portion of the benefit can be achieved with a 2 hours storage capacity, in all cases, and in terms of discounted payback period, 2 hours storage is the best option. The investment is less efficient under the assumption of interconnected operation at low fuel prices.

5. CONCLUSIONS

An energy management system (EMS) for the flexible operation of thermal power stations based on generation-integrated thermal energy storage (TES) has been proposed. The concept is applied on an existing 50-MW oil-fired Rankine-cycle power station. The possibilities of steam extraction before the high-pressure turbine (HPT) of the power station during off-peak demand have been investigated. Steam is extracted from the power station during off-peak demand for the charging of thermal tanks that contain suitable phase-change materials (PCMs). When power is required and/or it is cost-effective the tanks act as heat sources of secondary thermal power, for example as evaporators of organic Rankine cycle (ORC) plants that are suitable for power generation at reduced temperatures and smaller scales. This type of solution offers greater flexibility than TES-only technologies that store thermal energy and then release this back to the base power station, since it allows both derating and over-generation compared to the base power-station rating. Simulations of the operation of the power system of Crete for a number of scenarios indicate the potential benefits of the installation of TES, especially in the case of high fuel costs, high demand and autonomous operation of the system in which the payback period is 5 years, while they are reduced for interconnected operation, low fuel prices and low demand. In future work, we intend to investigate additional EMS strategies for the provision of ancillary services in transmission networks of smart grids. We intend to consider such strategies for increasing the thermal efficiencies of the secondary power stations during peak demand. The design requirements for fast-start plants in relation to the initial capital and operations and maintenance costs for the various levels of fast-start capability is nowadays common practice. We also aim to investigate fast-start secondary power plants with aggressive hot starts (reportedly within 10 min, and down to 10 s when the plants are at temperature). Such improvements can offer significant benefits to utilities in terms of primary and secondary frequency responses.

REFERENCES

[1] K. Roth, V. Scherer, K. Behnke, 2005, Enhancing the dynamic performance of electricity production in steam power plants by the integration of transient waste heat sources into the feed-water pre-heating system, *Int. J. Energy Technol. Policy*, vol. 3, pp. 50-65.

[2] M. Richter, F. Starinski, A. Starinski, G. Oeljeklaus, K. Gorner, 2015, Flexibilization of coal-fired power plants by dynamic simulation, *Proc. 11th Int. Modelica Conf*.

[3] M. J. Moran, H. N. Shapiro, 1999, Vapor Power Systems, in *Fundamentals of Engineering Thermodynamics*, 4th Ed., John Wiley & Sons, USA, pp. 372-414.

[4] Central Electricity Generating Board (CEGB), 1971, Feed Water Heating Systems, in *Modern Power Station Practice*, 2nd Ed., Pergamon Press, Oxford, UK, pp. 131-213.

[5] P. Romanos, G. Takis, E. Voumvoulakis, G. Tsourakis, N. Hatziargyriou, 2018, Thermal Energy Storage Contribution to the Flexibility and Economic Operation of an Island Power System, *CIGRE Conference*, Paris, Aug. 26-31.

[6] T. Bauer, D. Laing, R. Tamme, 2010, Overview of PCMs for concentrated solar power in the temperature range 200 to 350 ^{o}C, *Adv. Sci. Technol*., vol. 74, pp. 272-277.

[7] C. N. Markides, 2015, Low-concentration solar-power systems based on organic Rankine cycles for distributed-scale applications: Overview and further developments, *Front. Energy Res*., vol. 3, pp. 47:1-16.

[8] Hellenic Electricity Distribution Network Operator S.A., 2017, [Online]. Available: https://www.deddie.gr/en/themata-tou-diaxeiristi-mi-diasundedemenwn-nisiwn/stoixeia-ekkathariseon-kai-minaion-deltion-mdn/miniaia-deltia-ape-kai-thermikis-paragwgis-sta-mi/2017

[9] Environmental Directive 2010/75/EU (IED). [Online]. Available: http://eur-lex.europa.eu/legal-content/EN/TXT/?uri=celex%3A32010L0075

[10] Environmental Directive 2015/2193/EU (MCPD). [Online]. Available: http://eur-lex.europa.eu/legal-content/IT/TXT/?uri=celex:32015L2193

[11] I. Dincer, M. A. Rosen, 2011, Energy Storage Systems, *Thermal Energy Storage – Systems and Applications*, 2nd Ed., John Wiley & Sons, USA, pp. 51-190.

[12] S. Lemmens, 2015, A perspective on costs and cost estimation techniques for organic Rankine cycle systems, *3rd Int. Semin. ORC Power Syst*., October 12-14, Brussels, Belgium.

ACKNOWLEDGEMENT

The authors would like to acknowledge the assistance given to them by Mr Alexios Sotiropoulos with Public Power Corporation S.A. (PPC), Mr James Bowers with Scottish and Southern Electricity Networks (SSE), Mr Richard Drew with Uniper, Mr Dimitrios Tsintzilonis with TERNA Qatar and Dr. Nikos Soultanis with Independent Power Transmission Operator S.A. (ADMIE).